Controlled Polymerization of DL-Lactide and ϵ-Caprolactone by Structurally Well-Defined Alkoxo-Bridged Di- and Triyttrium(III) Complexes

Bradley M. Chamberlain, Brian A. Jazdzewski, Maren Pink, Marc A. Hillmyer,* and William B. Tolman*

Department of Chemistry, University of Minnesota, 207 Pleasant St. SE, Minneapolis, Minnesota 55455

Received January 19, 2000; Revised Manuscript Received March 22, 2000

ABSTRACT: We have prepared the yttrium(III) alkoxides $[(L^{Me2})(HL^{Me2})Y_3(OCH_2C_6H_5)_4]$ (**3**) and $[(S\text{-}L^{Me})Y]_2\cdot 2(HOCH_2C_6H_5)$ (**1**·2BnOH) through treatment of two previously developed complexes with benzyl alcohol. Complex **3** possesses a novel cluster structure that appears to be retained in solution and is capable of polymerizing both DL-lactide (LA) and ϵ-caprolactone (CL). The polymerizations are controlled as evidenced by the linear nature of molecular weight versus conversion plots and [M]/[**3**] ratios. The kinetics of LA polymerization using **3** are first-order with respect to the monomer at low [LA]/[Y] ratios. The polymerization of CL is zero-order in monomer. Complex **1**·2BnOH possesses a dimeric structure previously seen in both the solid and solution state. However, the added presence of benzyl alcohol moieties in **1**·2BnOH increases the rate of LA polymerization and allows for control over the molecular weights of isolated polylactide, a feature unseen in earlier reported dimers. The complex **1**·2BnOH is not active for the polymerization of CL.

Introduction

The ring-opening polymerization of cyclic esters such as DL-lactide (LA) and ϵ-caprolactone (CL) provides access to a class of biodegradable polyesters whose homo- and copolymers have found numerous biomedical, pharmaceutical, and agricultural applications.[1] Trivalent lanthanide alkoxides are particularly efficient catalysts for the synthesis of both polylactide (PLA)[2,3] and polycaprolactone (PCL),[3,4] but judicious control of their reactivity has been difficult due to a lack of knowledge of precatalyst structure and/or an inability to systematically tune catalyst activity through ligand design. Thus, important objectives of current research include not only the development of lanthanide-based complexes capable of polymerizing LA and CL in a controlled manner but also the elucidation of relationships between the structure and activity of well-defined catalysts.

Recently, we reported a series of novel yttrium(III) complexes coordinated by multidentate ligands based upon a 1,4,7-triazacyclononane framework.[5] In particular, we found that the dimers **1** and **2** promoted the polymerization of LA under mild conditions (25 °C, CH_2Cl_2) and that both the rate of polymerization and the molecular weight of the resultant PLA were influenced by differences in the ligand substituents and/or the presence of coordinated water. Neither **1** nor **2**, however, allowed ready control of PLA molecular weights by variation in the monomer-to-catalyst ratio. In addition, it was difficult to obtain information on the initiation mechanism since neither **1** nor **2** produced PLA chains with identifiable end groups.

On the basis of literature precedent,[2b,c] we hypothesized that treatment of **1** and **2** with an exogenous low-molecular-weight alcohol would lead to the formation of new catalysts with discrete alkoxide initiating groups. Moreover, we anticipated that such treatment would lead to control of polymer molecular weight through simple variation of monomer-to-catalyst ratios. Here we report the results of treatment of **1** and **2** with benzyl alcohol (BnOH), including the synthesis and full characterization of a novel triyttrium complex derived from **2**. Both the cluster (**3**) and **1**·2BnOH are effective for the controlled polymerization of LA. In addition, **3** is an effective catalyst for the polymerization of CL, thus allowing the preparation of PLA−PCL block copolymers.

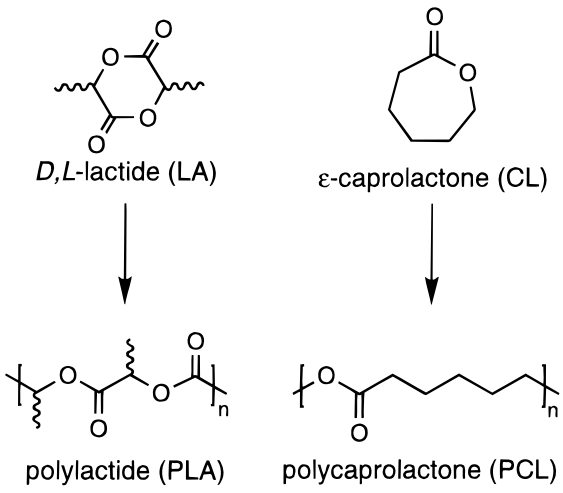

Results and Discussion

Synthesis and Characterization. Complexes **1**·2BnOH and **3** were prepared by sequential treatment of the appropriate ligand with 1 equiv of $Y[N(TMS)_2]_3$ followed by 1.1 equiv of BnOH (Schemes 1 and 2). Both complexes were isolated as colorless, crystalline solids in 38 and 70% yields (based on yttrium), respectively. X-ray diffraction analyses were performed on crystals

* To whom correspondence should be addressed. E-mail: hillmyer@chem.umn.edu; tolman@chem.umn.edu.

10.1021/ma0000834 CCC: $19.00
Published on Web 05/03/2000

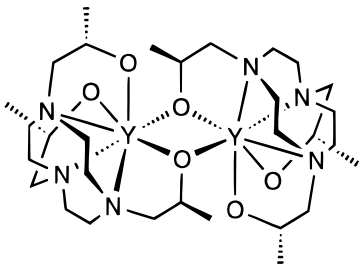

1

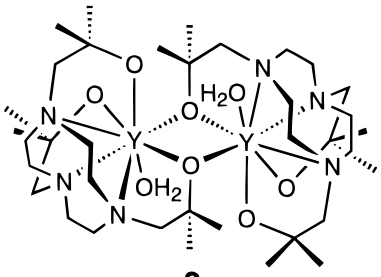

2

of both **1**·2BnOH (Figure 1) and **3** (Figure 2), and complete crystallographic data are included in the Supporting Information.

The crystal structure data confirmed that **1**·2BnOH comprises the previously characterized diyttrium complex **1** plus two molecules of benzyl alcohol. The complex crystallizes with two independent but chemically similar molecules in the asymmetric unit. On the basis of the ligand oxygen to benzyl alcohol oxygen distances [O(6)···O(1S) = 2.643(13) Å, O(5)···O(2S) = 2.670(10) Å], both benzyl alcohol molecules are hydrogen-bonded to the terminal η^1-alkoxides of one *S*-L^{Me} ligand in the first molecule. In the second molecule, each benzyl alcohol molecule is hydrogen-bonded to a terminal η^1-alkoxide of separate *S*-L^{Me} ligands [O(9)···O(3S) = 2.663(10) Å; O(10)···O(4S) = 2.699(8) Å]. In neither case do the benzyl alcohol molecules interact directly with the yttrium ions. Consequently, the Y_2(*S*-L^{Me})$_2$ units in the X-ray structures with and without included benzyl alcohol are the same, and key bond distances and angles in **1**·2BnOH are within experimental error of those in **1**.[5]

Scheme 1

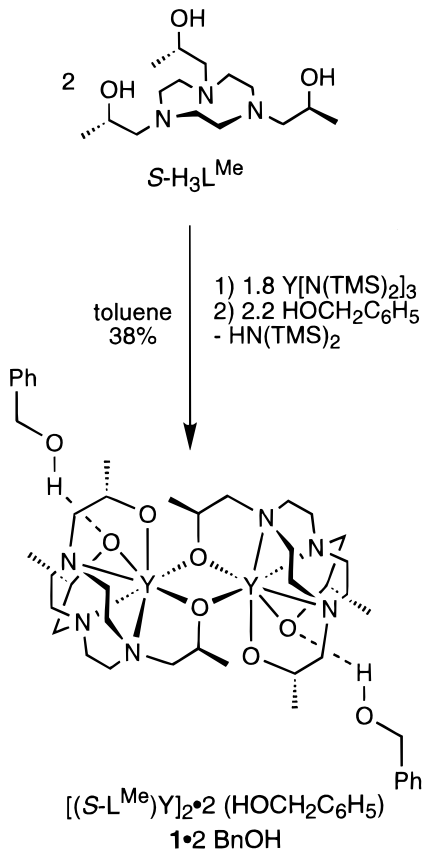

Scheme 2

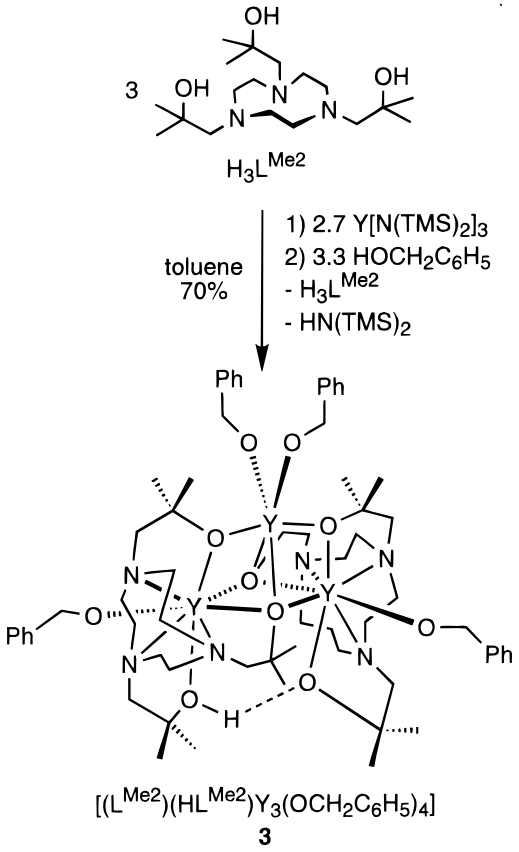

^{1}H NMR spectroscopic data for **1**·2BnOH in CD_2Cl_2 are consistent with retention of the dimeric unit in solution. Thus, **1** and **1**·2BnOH exhibit identical spectra, with the exception of peaks due to benzyl alcohol in the latter. Evidence in support of retention of the C_2-symmetric dinuclear structures in solution includes the presence of three doublets (J = 6 Hz) between 1.0 and 1.4 ppm, one for each methyl group per symmetry-related ligand.

X-ray diffraction analysis revealed that **3** is structurally quite different from **1**, **2**, and **1**·2BnOH. Complex **3** is a novel triyttrium complex with two different coordination environments for the three yttrium ions. Atoms Y1 and Y1A are both eight-coordinate, and each possesses a distorted triangulated dodecahedral coordination geometry. In contrast, Y2 is coordinated to six atoms in a distorted octahedral array. Atoms Y1 and Y1A are ligated by both nitrogen and oxygen donors, and Y2 is coordinated only to alkoxide ligands. Unlike **1**·2BnOH, the benzyl groups from BnOH are coordinated as alkoxides. Two benzyl alkoxides are ligated to Y2, one benzyl alkoxide is ligated to Y1, and one benzyl alkoxide is ligated to Y1A. The yttrium ions in **3** are bridged by four alkoxides to form a Y_3O_4 core. The two halves of the Y_3O_4 core (Figure 2b) are related by a

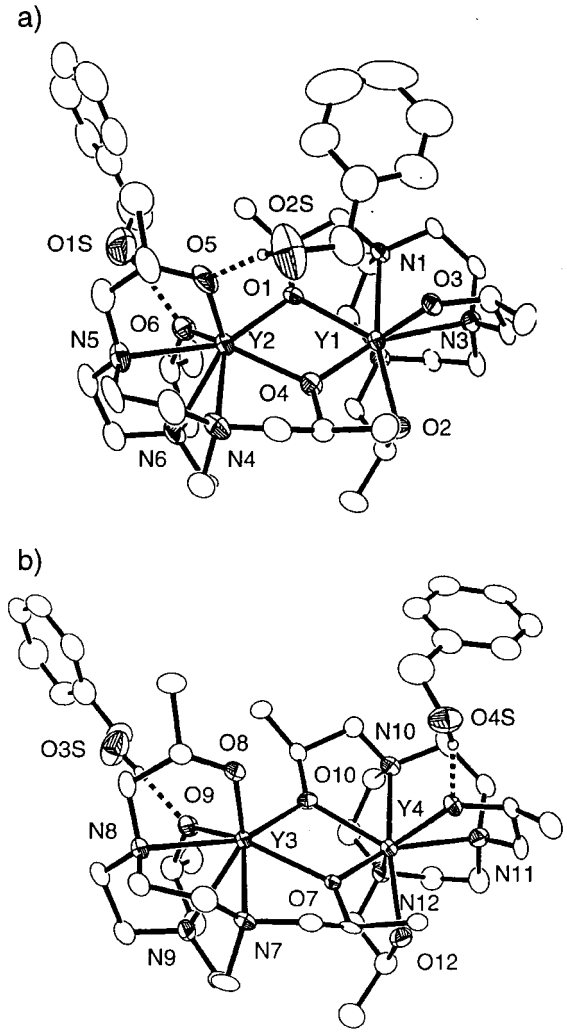

Figure 1. Representation of the two independent molecules in the X-ray crystal structure of **1**·2BnOH (50% ellipsoids, all hydrogen atoms except those involved in hydrogen bonds omitted for clarity; dashed lines indicate postulated hydrogen bonds) with (a) both benzyl alcohol molecules hydrogen-bonded to one *S*-L^{Me} ligand and (b) each benzyl alcohol molecule bonded to a separate *S*-L^{Me} ligand.

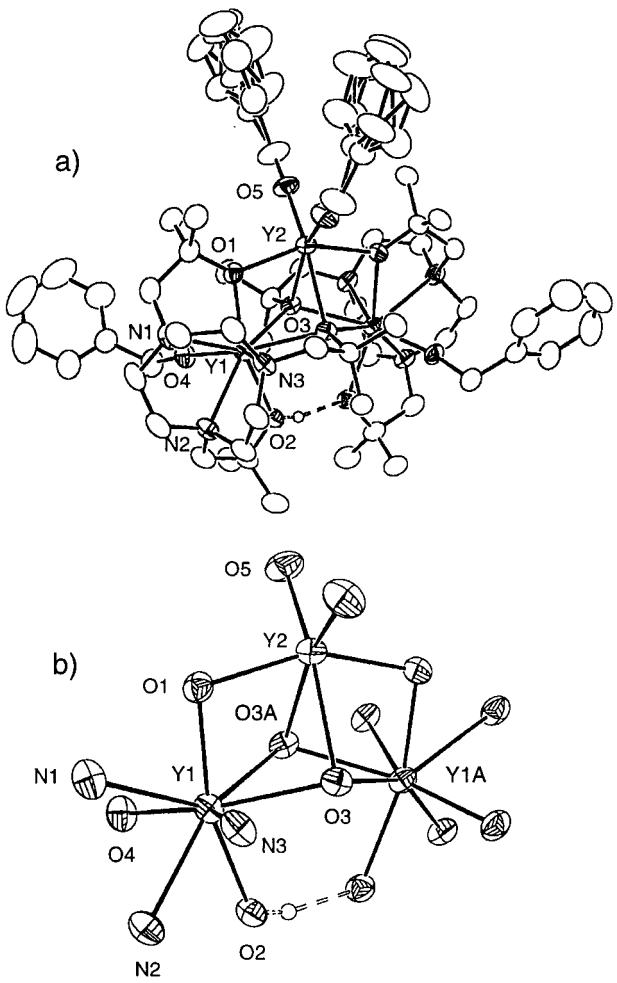

Figure 2. Representation of the X-ray crystal structure of **3** (50% ellipsoids, all hydrogen atoms except those involved in hydrogen bonds omitted for clarity; dashed lines indicate postulated hydrogen bonds) with (a) the full structure and (b) the $Y_3N_6O_{10}H$ core.

C_2-rotational axis through Y2 and perpendicular to the line defined by O3 and O3A. The alkoxides that make up the Y_3O_4 core are from the two L^{Me2} ligands, each contributing two of its three alkoxides for bridging. One pair of alkoxides bridges Y1(Y1A) and Y2, and the remaining pair of alkoxides bridges Y1(Y1A), Y1A(Y1), and Y2. Average Y−O distances for the η^2- and η^3-bridges are 2.28 and 2.50 Å, respectively, and the resultant Y1···Y2 and Y1···Y1A distances are 3.504(3) and 4.197(4) Å, respectively. The third alkoxide of each L^{Me2} ligand participates in a η^1-bond with Y1 or Y1A, with an average Y−O distance of 2.35 Å.

We hypothesize that the novel cluster geometry of **3** is retained in solution, as deduced from the pattern of sharp resonances in the ^{1}H NMR spectrum (Figure 3). Importantly, there are five singlets between 1.8 and 1.1 ppm in a 2:1:1:1:1 ratio, corresponding to the six methyl groups in half of the symmetrical $Y_3(L^{Me2})_2$ subunit. Supporting the retention of the C_2-symmetric triyttrium complex structure in solution are two benzylic resonances in a 1:1 ratio at 5.06 (singlet) and 4.97 ppm (AB quartet), respectively. We attribute the singlet to the two symmetry-related benzyl alkoxides connected to Y2 and the AB quartet (J = 12, 3 Hz) to the two symmetry-related benzyl alkoxides ligated to Y1 and Y1A. The absence of geminal coupling in the signal at 5.06 ppm may be due to rapid interchange of the *cis*-benzyl alkoxides on Y2. Of note, these two alkoxides are disordered in the X-ray crystal structure of **3**.

One alcohol proton must be present in order for **3** to remain charge neutral as indicated by the X-ray crystal structure. This proton is observed as a sharp resonance at 14.18 ppm in the ^{1}H NMR spectrum (Figure 3). Attempts to determine the connectivity of the proton by two-dimensional ^{1}H NMR techniques were unsuccessful. This proton was not found crystallographically but was placed on O2 on the basis of bond angles and distances. Other choices for placement of the proton included O4 and O5, but these were ruled out on the basis of both their shorter Y−O bond lengths [Y1−O2 = 2.347(2) Å, Y1−O4 = 2.145(2) Å, Y2−O5 = 2.101(2) Å] and their Y−O−C angles [Y1−O2−C12 = 122.1(2)°, Y1−O4−C25 = 170.9(2)°, Y2−O5−C32 = 172.1(2)°]. The proton was placed between O2 and O2A (which are 2.525(2) Å apart) in a hydrogen-bonded position, disordered (1:1) with respect to its symmetry-equivalent position.

Polymerization of DL-Lactide. Complex **3** is active for the polymerization of LA and displays polymerization rates between those of **1** and **2** at fixed [LA]/[Y] ≈

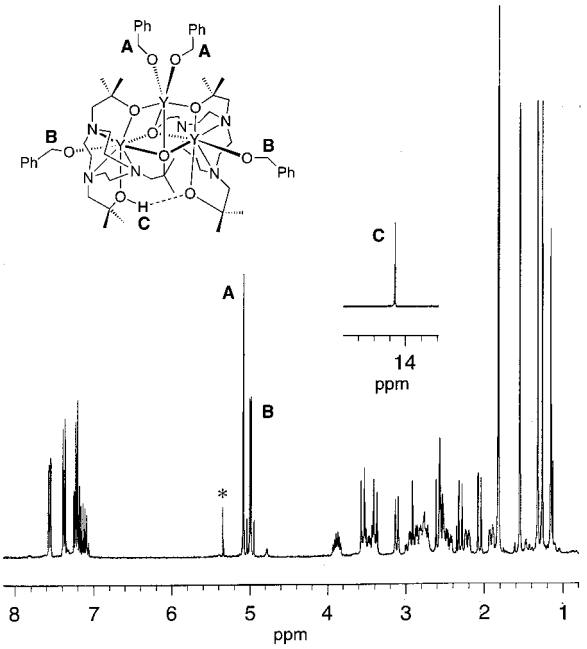

Figure 3. ^{1}H NMR spectrum of **3** in CD_2Cl_2 at 25 °C. The * denotes a resonance associated with the solvent.

150 (Y = yttrium center) (Table 1). The end groups of PLA produced by **3** were benzylalkoxycarbonyl units as determined by ^{1}H NMR spectroscopy. Thus, benzyl alkoxide moieties in **3** were incorporated into the polymer chains, consistent with a polymerization that proceeds by a coordination−insertion mechanism.[2c] At fixed [LA]/[Y], molecular weights of the polymers prepared with **3** were generally lower than those of the polymers obtained at comparable yields with **1** and **2**. However, M_w/M_n ratios (PDIs) of the polymers produced by **3** were significantly smaller than of those prepared with **1** and **2**.[6] Unlike **1** and **2**, the polymerization of LA with **3** exhibited a linear relationship between polymer molecular weight (M_n) and monomer conversion (Figure 4).

The linear nature of the data in Figure 4, in combination with the low PDI values, suggest the polymerization of LA by **3** is controlled. However, size exclusion chromatography (SEC) analysis indicated that **3** is also an effective transesterification catalyst. Although SEC traces of the polymers prepared with **3** at [LA]/[Y] ≈ 150 were unimodal up to 68% conversion, they began to show bimodal peaks at conversions greater than 75% (Figure 5). Moreover, SEC traces of polymers prepared with **3** at higher [LA]/[Y] ratios (e.g., 450 and 1000) were distinctly bimodal, even at lower conversions. These observations are consistent with the predicted effects of transesterification processes in lactone polymerizations. If transesterification effectively competes with ring-opening polymerization, the PDIs of resultant polymers should broaden with increasing conversion, and molecular weight distributions may be bimodal.[7]

The number of active initiating sites in **3** for the polymerization of LA also was determined (Table 2). At fixed conversion (≈97%), the degree of polymerization (i.e., number of repeat units) was plotted as a function of the [LA]/[**3**] ratio (Figure 6). Because the plot in Figure 6 is linear, the average number of initiating sites in **3** is simply the inverse of the slope of the fitted line (0.4).[2c] Thus, **3** has on average 2.5 ± 0.2 (of a possible 4)[8] initiation sites per complex. The observation that **3** does not utilize all of its possible active sites has precedent in related lanthanide alkoxide chemistry. For example, McLain reported that $Y(OCH_2CH_2NMe_2)_3$ utilized only two of its three alkoxide ligands for the polymerization of LA.[3a] At this point we are not certain why **3** exhibits a nonintegral number of initiating sites.

Table 1. Representative Polymerizations of LA at [LA]/[Y] ≈ 150 in CH_2Cl_2 at 25 °C[a]

entry	complex	t (h)	yield (%)	M_n (×10^3)	M_w/M_n
1	**1**	48	88	20.9	1.31
2	**2**	0.03	90	66.9	1.62
3	**3**	12	75	8.7	1.15
4	**1**·2BnOH	24	80	9.7	1.23

[a] For details on the polymerization procedure, see the Experimental Section.

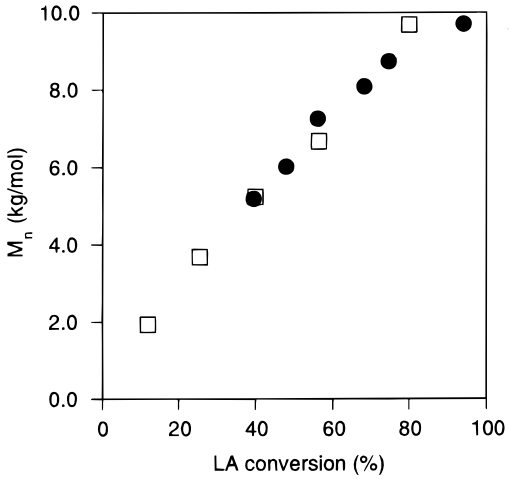

Figure 4. Plot of PLA M_n (vs polystyrene standards) as a function of conversion at 25 °C in CH_2Cl_2 at ([M]/[Y] ≈ 150) using **3** (●) and **1**·2BnOH (□).

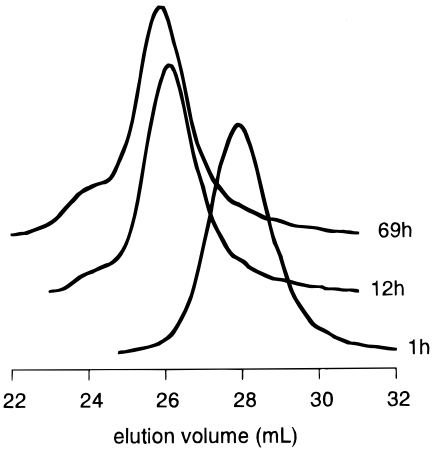

Figure 5. SEC traces of isolated PLA produced by **3** ([LA]/[Y] ≈ 150) at 1, 12, and 69 h. Monomer conversions are 39, 75, and 94%, respectively; PDI values are 1.10, 1.15, and 1.20, respectively.

Conversions of LA with time at various concentrations of **3** in CD_2Cl_2 at 22 °C were monitored by ^{1}H NMR spectroscopy until the equilibrium monomer concentration was reached ($[LA]_{eq}$ = 0.047 M).[9] Of the three polymerizations examined, first-order kinetics in monomer were observed only at [LA]/[Y] ≈ 50. The appropriate semilogarithmic plot of conversion vs time for this polymerization is shown in Figure 7. The kinetics of polymerizations performed at [LA]/[Y] ≈ 70 and 150 were complicated. Conversion data in these polymeriza-

Table 2. Determination of the Number of Active Initiating Sites in 3[a]

entry	monomer	[M]/[Y][b]	M_n ($\times 10^3$)[c]	M_w/M_n
1	LA	20.7	3.4	1.54
2	LA	30.0	4.2	1.40
3	LA	41.5	7.3	1.32
4	LA	62.3	10.0	1.2
5	LA	82.3	14.2	1.23
6	CL	19.6	3.1[d]	1.31
7	CL	30.1	5.5[d]	1.48
8	CL	40.4	9.0[d]	1.57
9	CL	60.2	12.4[d]	1.77
10	CL	79.6	17.5[d]	1.74

[a] Polymerizations were run in CH_2Cl_2 at 25 °C for 16 h; isolated yields were >97%. [b] M = monomer; Y = yttrium center. [c] Determined by ^{1}H NMR spectroscopy in $CDCl_3$. [d] Oligomers were observed by SEC.

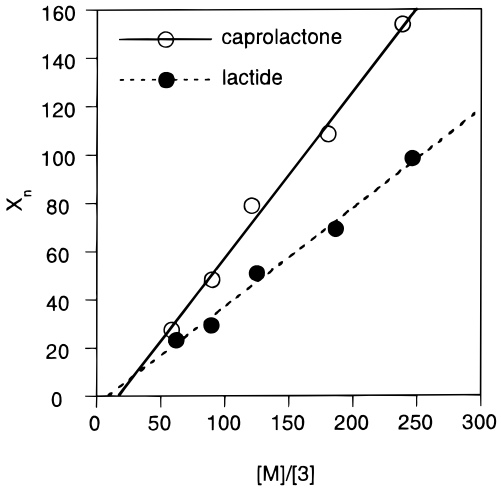

Figure 6. Plot of the degree of LA and CL polymerization (i.e., number of repeat units) vs [M]/[**3**] at 25 °C in CH_2Cl_2 (t = 16 h). The dashed line represents the linear fit of PLA experimental data; the solid line represents the linear fit of PCL experimental data (R = 0.996).

tions could only be fitted to higher-order exponential expressions involving two first-order rate constants separated by an order of magnitude in value. These complexities and unsuccessful initial rate experiments prevented us from determining the order in initiator for **3** and, consequently, an accurate value for the second-order propagation rate constant. Under the conditions used for the kinetics shown in Figure 7, the apparent first-order rate constant k_{app} is 8.2 × 10^{-4} s^{-1}.

Complex **1**·2BnOH also is an active LA polymerization catalyst. The end groups of the PLA polymers produced by **1**·2BnOH were determined by ^{1}H NMR spectroscopy, and only benzylalkoxycarbonyl end groups were observed. Thus, the benzyl alkoxide moieties in **1**·2BnOH were incorporated into the polymer chains, again consistent with a polymerization that proceeds by a coordination−insertion mechanism.[2c] Both the molecular weights and the PDIs of the polymers prepared with **1**·2BnOH were comparable to those obtained with **3** at similar yields. In addition, like complex **3**, **1**·2BnOH exhibited a linear relationship between polymer molecular weight (M_n) and monomer conversion (Figure 4). The linear nature of this plot, in combination with low PDI values, suggests that the polymerization of LA by **1**·2BnOH also is controlled.

Interestingly, from Figure 4 the slopes of the lines for **3** and for **1**·2BnOH are similar. This observation is

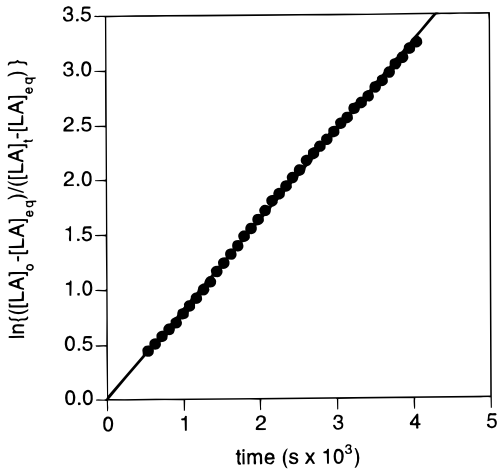

Figure 7. Semilogarithmic plot of LA conversion with time in CD_2Cl_2 at 22 °C using **3** as initiator ($[LA]_0$ = 0.700 M, [LA]/[Y] ≈ 50, [**3**] = 4.96 mM). The solid line represents the linear fit of experimental data (R = 0.999).

consistent with approximately two initiating sites per **1**·2BnOH, a conclusion we base on the following reasoning. The slopes of the lines given in Figure 4 represent changes in average polymer molecular weights with respect to the changes in lactide conversion. Since the [LA] is fixed in these polymerizations, the rate of molecular weight change is determined by the total number of chains the monomer must be distributed between; the more chains, the slower the average molecular weight increase, and the smaller the slope. The number of polymer chains is set by [I], the concentration of active initiating sites. In turn, [I] is set by the concentration of the complex used as an initiator and its average number of initiating sites. From Figure 6 we determined that there were approximately 2.5 initiating sites per **3**, so at [LA] = 1 M, [LA]/[Y] ≈ 150, [Y]/[**3**] = 3, and [I]/[**3**] ≈ 2.5, we calculate [I] in the polymerizations initiated with **3** to be ≈5.6 mM [(1 M/150/3) × 2.5]. Since the slope of the data in Figure 4 for **1**·2BnOH is the same as that for **3**, within error, then [I] for each is also the same. Thus, for **1**·2BnOH with [LA] = 1 M, [LA]/[Y] ≈ 150, and [Y]/[**1**·2BnOH] = 2, we calculate [I]/[**1**·2BnOH] to be 1.7 [(0.0056 M × 2 × 150)/1 M]. Therefore, although we do not have accurate molecular weight measurements as a function of [LA]/[**1**·2BnOH] ratios, the data in Figure 4 are consistent with slightly less than two initiating sites per **1**·2BnOH.

In preliminary experiments, the conversion of LA with time using **1**·2BnOH in CD_2Cl_2 at 22 °C was monitored by ^{1}H NMR spectroscopy until the equilibrium monomer concentration was reached ([LA]/[Y] ≈ 150).[10] Like **3**, the polymerization of LA by **1**·2BnOH is apparently first-order in monomer, with an observed first-order rate constant (k_{app}) under these conditions of 4.5 × 10^{-5} s^{-1}. Assuming that the polymerization proceeds according to the simple overall kinetic scheme described for **3**, **1**·2BnOH is about 20 times slower than **3** at a fixed [LA]/[Y] of ≈150.

Polymerization of ϵ-Caprolactone. Although both complexes **1** and **1**·2BnOH were inactive for the polymerization of CL, complex **3** is active for this monomer and displayed rates that were much faster than those of **2** at fixed [CL]/[Y] ≈ 150 (Table 3). The end groups of PCL materials produced by **3** were determined by ^{1}H NMR spectroscopy to be benzylalkoxycarbonyl units. Thus, as in the LA polymerizations, the benzyl alkoxide

Table 3. Polymerization of CL at [CL]/[Y] ≈ 150 in CH_2Cl_2 at 25 °C[a]

entry	complex	time (h)	yield (%)	M_n ($\times 10^3$)	M_w/M_n
1	**2**	72	15	33.7	1.50
2	**3**	1	100	5.6[b]	1.31
3	**3**	2	100	11.8[b]	1.22
4	**3**	4	98	19.0[b]	1.24
5	**3**	6	100	20.1	1.6

[a] For details on the polymerization procedure, see the Experimental Section. [b] Oligomers were observed by SEC.

moieties in **3** were incorporated into the polymer chains, consistent with a polymerization that proceeds by a coordination−insertion mechanism.[2c] Although ^{1}H NMR analysis indicated that the polymerization of CL by **3** was complete within 1 h,[11] SEC traces of isolated polymers exhibited significant oligomeric fractions up to reaction times of 6 h. During this time period, both the M_n and the PDIs of isolated PCL increased steadily. After a reaction time of 6 h, however, no oligomers were observed by SEC, and the M_n remained relatively constant. Complex **3** appears to be effective for transesterification (intramolecular and intermolecular) in the polymerization of CL.

The number of active initiating sites in **3** for the polymerization of CL was also determined (Table 2). At fixed conversion,[12] the degree of polymerization was plotted as a function of the [CL]/[**3**] ratio (Figure 6). From the slope of the line fitted to the data (0.65) **3** exhibits, on average, 1.5 ± 0.1 active CL polymerization sites per catalyst,[2c] which contrasts with the 2.5 active sites per **3** determined for the polymerization of LA. The observation of monomer dependence on the number of initiating sites in the polymerization of LA and CL has been reported for $Al(O^iPr)_3$.[13]

The observation that **3** possesses different average numbers of active sites for the polymerization of LA and CL suggests that these polymerizations proceed by different mechanisms. This notion was corroborated by the results of kinetics experiments. Conversions of CL with time at various concentrations of **3** in CD_2Cl_2 at 22 °C were monitored by ^{1}H NMR spectroscopy ([CL]/[Y] ≈ 50, 70, 90, and 150). In each case the polymerization was apparently zero-order in monomer, even up to 75% conversion (Figure 8). Therefore, the polymerization of CL by **3** presumably proceeds according to

$$\frac{-\mathrm{d[CL]}}{\mathrm{d}t} = k_{app}[\mathrm{CL}]^0$$

where $k_{app} = k_p[\mathrm{I}]^m$, and k_p is the propagation rate constant. Determination of the propagation rate constant is complicated by the possible aggregation of the active species during the polymerization.[14] To determine the order in initiator (m), log k_{app} was plotted versus log [**3**] (Figure 9). From this plot, the order in initiator (slope) is 0.47 ± 0.06. Thus, the polymerization of CL by **3** proceeds according to the overall kinetic law of the form

$$\frac{-\mathrm{d[CL]}}{\mathrm{d}t} = k_p[\mathbf{3}]^{1/2}$$

According to a preliminary report by McLain, the polymerization of LA using a lanthanide alkoxide also was zero-order in monomer. He suggested that the observed kinetics result from a Y(III) center that was presaturated with coordinated lactide, and the rate-determining step involves reaction of a yttrium alkoxide ligand with a coordinated lactide.[3a] The half-order dependence on [**3**] in the polymerization of CL suggests aggregation of an active species derived from **3** during the reaction. Fractional dependencies upon initiator have been observed for the polymerization of CL with related aluminum alkoxides; in these systems, studies indicate that the observed kinetics result from active species aggregation in the polymerization medium.[15] Thus, despite evidence that **3** retains its monomeric form in the absence of lactone, kinetic evidence suggests that propagating species derived from it dimerize during the polymerization of CL.

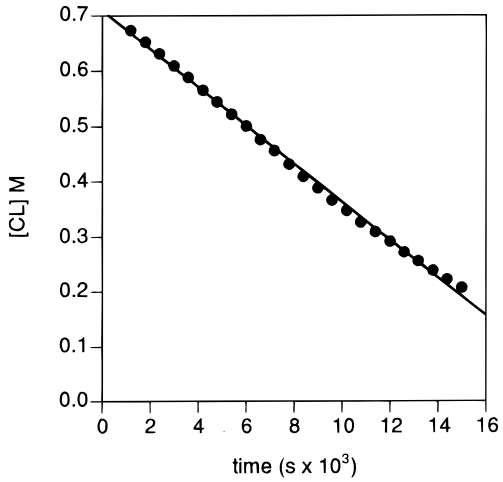

Figure 8. Plot of CL conversion with time in CD_2Cl_2 at 22 °C using **3** as initiator ($[CL]_0 = 0.700$ M, [CL]/[Y] ≈ 150, [**3**] = 1.56 mM). Only every fifth data point is shown for clarity. The solid line represents the linear fit of experimental data ($R = 0.999$) and $k_{app} = 3.5 \times 10^{-5}$ s^{-1}.

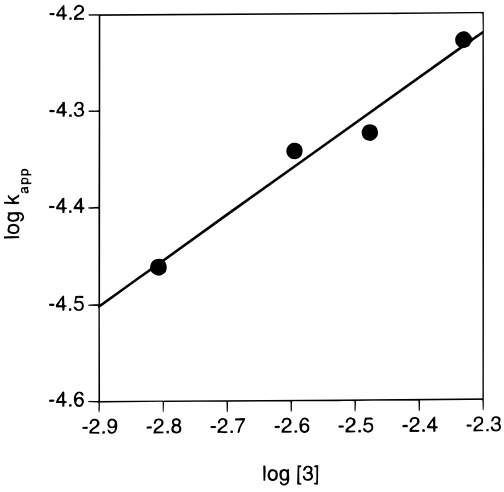

Figure 9. Plot of log k_{app} vs log [**3**] for the polymerization of CL using **3** as initiator ($[CL]_0 = 0.700$ M). The solid line represents the linear fit of experimental data ($R = 0.986$).

Synthesis of PLA−PCL Block Copolymers. In preliminary experiments, we have found **3** to be a capable catalyst for the preparation of PCL−PLA block copolymers (Table 4). Sequential treatment of **3** with these two monomers leads to a block copolymer (entry 1, Table 4). The polymerization yield, with a reaction time of 6 h for the CL polymerization and 12 h for the LA polymerization, was quantitative for CL and 80% for LA. The molecular weight of this block copolymer by SEC analysis was greater than expected if the two

Table 4. Copolymerization of CL and LA with 3 in CH_2Cl_2 at 25 °C[a]

entry	[CL]/[Y]	[LA]/[Y]	*t*(CL/LA) (h/h)[b]	conversion (CL/LA) (%/%)[c]	M_n ($\times 10^3$)	M_w/M_n
1	150	150	6/12	100/80	30.0	1.63
2	150	150	1/17	43/57	15.6[d]	1.24
3	150	150	18[e]	0/30		

[a] For details on the polymerization procedure, see the Experimental Section. [b] Reaction time of CL/Reaction time of LA. [c] Conversion of CL/Conversion of LA. [d] Oligomers were observed by SEC. [e] CL and LA added simultaneously.

monomers had polymerized separately, but further analysis is necessary to definitively rule out homopolymer contamination. In contrast, if the initial reaction time for CL was reduced to 1 h, SEC analysis showed one narrow polymer peak, one broad peak comprising a cluster of small-molecule oligomers, and residual monomer (entry 2, Table 4). If CL and LA were added simultaneously, only polylactide was isolated (entry 3, Table 4). This is consistent with a slow crossover reaction between a PLA propagating species and CL.

Summary and Perspective

In conclusion, we have discovered an alkoxo-bridged triyttrium(III) complex (**3**) with a novel cluster structure that is retained in solution (albeit with kinetic evidence for aggregation during the polymerization of CL). This cluster is an effective initiator for the polymerization of LA and CL. Analysis of the LA polymerizations suggested that the polymerization is first-order in monomer and proceeds in a controlled fashion. The polymerization of CL, however, is less controlled (cf., the formation of cylic oligomers and higher PDIs) and is zero-order in monomer. In addition, **3** is effective for the synthesis of a PLA−PCL block copolymer even though it possesses different numbers of active initiating sites for each monomer. We have also modified the catalytic activity of a diyttrium(III) complex reported earlier[5] through the addition of benzyl alcohol (**1**·2BnOH). Such treatment does not disrupt the dimeric structure previously seen in either the solid or solution state but does increase its rate of polymerization of LA. This modified dimer also shows control over the PLA molecular weights of isolated LA polymers.

Our studies show that systematic changes in the structure of discrete Y-based complexes can lead to significant changes in their lactone polymerization activity. We have made progress in understanding the kinetics, number of initiating sites, aggregation phenomena, and active structure identity in these active catalysts. However, aggregation and cluster formation in these Y-based complexes complicates their polymerization behavior. Obviating these problems through the development of new well-defined catalysts remains an important research objective.

Experimental Section

General Procedures. All reagents were obtained from commercial sources and used as received unless otherwise noted. All solvents were purchased from commercial sources and dried under N_2 by standard methods immediately before use.[16] All air-sensitive reactions were performed either in a Vacuum Atmospheres glovebox under an N_2 atmosphere or by using standard Schlenk and vacuum-line techniques. NMR experiments were carried out on a Varian VXR-500, VXR-300, or VI-300 spectrometer using standard parameters. ^{1}H NMR chemical shifts are reported versus tetramethylsilane and referenced to the residual solvent peaks. FTIR spectra were collected on a Mattson Polaris spectrophotometer. Fast atom bombardment (FAB) mass spectra were obtained on a VG-707E-HF mass spectrometer using xenon gas for ionization. Elemental analyses were determined by Atlantic Microlabs, Norcross, GA. Molecular weights (M_w and M_n) and polydispersities (M_w/M_n) were determined by size exclusion chromatography (SEC) with respect to polystyrene standards. All samples were analyzed at 40 °C using a Hewlett-Packard high-pressure liquid chromatograph equipped with three Jordi polydivinylbenzene columns of 104, 103, and 500 Å pore sizes and a HP1047A refractive index detector, using THF as the eluent with a flow rate of 1 mL min^{-1}. Commercial LA was sublimed prior to use. CL was dried over CaH_2 and then distilled under N_2. H_3L^{Me2} and *S*-H_3L^{Me} were synthesized using published procedures.[5] $Y[N(TMS)_2]_3$ was purchased from Alfa Aesar. Glassware used for polymerization reactions was pretreated with a 1 M solution of dichlorodimethylsilane and then flame-dried under vacuum.

[(*S*-L^{Me})Y]$_2$·2(HOCH$_2$C$_6$H$_5$) (1·2BnOH). The compounds *S*-L^{Me} (0.092 g, 0.30 mmol) and $Y[N(TMS)_2]_3$ (0.156 g, 0.273 mmol) were stirred in toluene (5 mL) for 18 h. Benzyl alcohol (1.00 mL of a 0.387 M solution in toluene) was then added, and the solution was allowed to stir an additional 18 h. The solution was then concentrated to less than 1 mL, and colorless blocks of **1**·2BnOH crystallized over the course of 2 h (0.052 g, 0.052 mmol, 38%). Mp > 250 °C; $[\alpha]^{20}_D = +50 \pm 0.6$ ($c = 4.8 \times 10^{-3}$ g/mL, CH_2Cl_2). IR (KBr): 2954, 2912, 2878, 2828, 2576, 1488, 1460, 1334, 1306, 1150, 1081, 1032, 996, 940, 856 cm^{-1}. ^{1}H NMR (300 MHz, CD_2Cl_2): δ 0.98 (d, $J = 6$ Hz, 6H), 1.02 (d, $J = 6$ Hz, 6H), 1.34 (d, $J = 6$ Hz, 6H), 2.29−2.67 (m, 22H), 2.75 (dd, $J = 12$, 3 Hz, 2H), 2.91−3.23 (m, 10H), 3.34−3.45 (m, 2H), 4.14−4.25 (m, 6H), 4.70 (s, 4H), 7.10−7.40 (m, 10H) ppm. Anal. Calcd for $C_{44}H_{76}N_6O_8Y_2$: C, 53.11; H, 7.70; N, 8.45. Found: C, 53.32; H, 7.66; N, 8.56.

[(L^{Me2})(HL^{Me2})Y$_3$(OCH$_2$C$_6$H$_5$)$_4$] (3). The compounds L^{Me2} (0.1387 g, 0.40 mmol) and $Y[N(TMS)_2]_3$ (0.2065 g, 0.36 mmol) were stirred in toluene (5 mL) for 18 h. Benzyl alcohol (0.94 mL of a 0.387 M solution in toluene) was then added, and the solution was allowed to stir an additional 18 h. The solution was then concentrated to less than 1 mL, and colorless blocks of **3** crystallized over the course of 2 h (0.117 g, 0.085 mmol, 70%). Mp > 250 °C. IR (KBr): 3443 (br, OH), 2838 (br), 1498, 1456, 1383, 1367, 1204, 1167, 1099, 1041, 968 cm^{-1}. ^{1}H NMR (300 MHz, CD_2Cl_2): δ 1.13 (s, 6H), 1.24 (s, 6H), 1.30 (s, 6H), 1.52 (s, 6H), 1.79 (s, 12H), 1.9−3.9 (m, 36H), 4.97 (dd, $J = 12$, 3 Hz, 4H), 5.06 (s, 4H), 7.02−7.24 (m, 10H), 7.32−7.38 (m, 5H), 7.50−7.56 (m, 5H), 14.18 (s, 1H) ppm. Anal. Calcd for $C_{64}H_{101}N_6O_{10}Y_3$: C, 55.65; H, 7.37; N, 6.08. Found: C, 54.51; H, 7.39; N, 6.03.

General Homopolymerization Procedure. A 25 mL Schlenk flask was charged with a 5 mM solution of the catalyst in CH_2Cl_2. To this solution was added a 1 M solution of monomer in CH_2Cl_2. After stirring under an atmosphere of N_2 for the appropriate amount of time, the reaction was quenched with 1 M HCl (4 drops). Following removal of the solvent under vacuum, the polymer mixture was taken up in $CDCl_3$ (3 mL) and then subjected to analysis by ^{1}H NMR spectroscopy and SEC.

General Copolymerization Procedure. A 25 mL Schlenk flask was charged with a 5 mM solution of the catalyst in CH_2Cl_2. To this solution was added a 1 M solution of CL in CH_2Cl_2. After stirring under an atmosphere of N_2 for the appropriate amount of time, a 1 M solution of LA in CH_2Cl_2 was added. Following another period of stirring under N_2, the reaction was quenched with 1 M HCl (4 drops). Following removal of the solvent under vacuum, the polymer mixture was taken up in $CDCl_3$ (3 mL) and then subjected to analysis by ^{1}H NMR spectroscopy and SEC.

General Kinetic Procedure. In the glovebox, exactly 2 mL of a 0.700 M solution of monomer in CD_2Cl_2 was added to the appropriate amount of solid catalyst. After mixing for approximately 10 s, the resulting solution was transferred to a NMR tube, which was then capped and wrapped with Parafilm. The NMR tube was then placed in the probe of a 300 MHz Varian VXR NMR spectrometer whose temperature

had been set and regulated to 22 °C. The polymerization reaction was monitored using a preaquisition delay protocol, with each data acquisition having one transient. Conversions were determined by relative integration of the monomer and polymer resonances.

X-ray Crystallography. [(*S*-L^{Me})Y]$_2$·2($HOCH_2C_6H_5$) (1·2BnOH). A colorless block crystal was attached to a glass fiber with heavy-weight oil and mounted on a Siemens SMART system for data collection at 173(2) K. An initial set of cell constants was calculated from reflections harvested from three sets of 20 frames. These initial sets of frames were oriented such that orthogonal wedges of reciprocal space were surveyed. This produced orientation matrices from 248 reflections. Final cell constants were calculated from a set of 6193 strong reflections from the actual data collection. A randomly oriented region of reciprocal space was surveyed to the extent of 1.3 hemispheres to a resolution of 0.84 Å. Three major swaths of frames were collected with 0.30° steps in ω.

The space group $P2_1$ was determined on the basis of systematic absences and intensity statistics.[17] A successful direct-methods solution was calculated which provided most non-hydrogen atoms from the E-map. Several full-matrix least-squares/difference Fourier cycles were performed which located the remainder of the non-hydrogen atoms. All non-hydrogen atoms were refined with anisotropic displacement parameters unless otherwise stated. All hydrogen atoms were placed in ideal positions and refined as riding atoms with individual (or group if appropriate) isotropic displacement parameters.

Two specimens were examined before data collection. The crystal chosen was cut in half prior to mounting. The asymmetric unit contains two dimers. Side-by-side comparison of these dimers showed only minor differences. A total of four benzyl alcohol molecules were found in the asymmetric unit, two associated with each dimer in different relative positions. All four benzyl alcohol OH protons were placed in ideal positions and refined as riding atoms.

[(L^{Me2})(HL^{Me2})Y_3($OCH_2C_6H_5$)$_4$] (3). A colorless plate was attached to a glass fiber with heavy-weight oil and mounted on a Siemens SMART system for data collection at 213(2) K. An initial set of cell constants was calculated from reflections harvested from three sets of 20 frames. These initial sets of frames were oriented such that orthogonal wedges of reciprocal space were surveyed. This produced orientation matrices determined from 125 reflections. Final cell constants were calculated from a set of 8192 strong reflections from the actual data collection. A randomly oriented region of reciprocal space was surveyed to the extent of 1.3 hemispheres to a resolution of 0.84 Å. Three major swaths of frames were collected with 0.30° steps in ω.

The space group *C*2/*c* was determined on the basis of systematic absences and intensity statistics.[17] A Patterson solution was calculated which provided the position of the metal atoms. Several full-matrix least-squares/difference Fourier cycles were performed locating all non-hydrogen atoms which were then refined with anisotropic displacement parameters. All hydrogen atoms were placed in ideal positions and refined as riding atoms with individual isotropic displacement parameters.

The structure was found to be a trimer (Y2 at a special position 0.5, *y*, 0.25 on a 2-fold axis) with a 2-fold axis in its center. One benzyl alcoholate molecule is disordered (major site occupancy 63%). On the basis of charge balance considerations, NMR data, and interatomic distances, a proton was placed on O2, 50% disordered with its symmetry-equivalent position.

Acknowledgment. Funding for this work was provided by the National Science Foundation (NYI award to W.B.T., Grant CHE-9207152 to W.B.T., and Grant CHE-9975357 to W.B.T. and M.A.H.). We thank Dr. Kate Aubrecht and Dr. Brendan O'Keefe for helpful discussions and a critical reading of this manuscript.

Supporting Information Available: Complete drawings and full details of the X-ray structure determinations, including tables of bond lengths and angles, atomic positional parameters, and final thermal parameters. This material is available free of charge via the Internet at http://pubs.acs.org.

References and Notes

(1) Recent references: (a) Mueller, H. M.; Seebach, D. *Angew. Chem., Int. Ed. Engl.* **1993,** *32*, 477. (b) Vert, M.; Li, S. N.; Spenlenhauer, G.; Guerin, P. J. *Pure Appl. Chem.* **1995,** *A32*, 787.

(2) (a) Le Borgne, A.; Pluta, C.; Spassky, N. *Macromol. Rapid Commun.* **1995,** *15*, 955. (b) Stevels, W. M.; Ankone, M. J. K.; Dijkstra, P. J.; Feijen, J. *Macromolecules* **1996,** *29*, 3332. (c) Stevels, W. M.; Ankone, M. J. K.; Dijkstra, P. J.; Feijen, J. *Macromolecules* **1996,** *29*, 6132. (d) Simic, V.; Spassky, N.; Hubert-Pfalzgraf, L. G. *Macromolecules* **1997,** *30*, 7338. (e) Yasuda, H.; Furo, M.; Yamamoto, H.; Nakamura, A.; Miyake, S.; Kibino, N. *Macromolecules* **1992,** *25*, 5115.

(3) (a) McLain, S. J.; Ford, T. M.; Drysdale, N. E. *Polym. Prepr. (Am. Chem. Soc., Div. Polm. Chem.)* **1992**, *33*, 463. (b) Simic, V.; Giradon, V.; Spassky, N.; Hubert-Pfalzgraf, L. G.; Duda, A. *Polym. Degrad. Stab.* **1998,** *59SI*, 222. (c) Zhang, J.; Gao, Z. H.; Zhong, Z. Y.; Jing, X. B. *Polym. Int.* **1998,** *45*, 60. (d) Miola-Delaite, C.; Hamaide, T.; Spitz, R. *Makromol. Chem. Phys.* **1999,** *200*, 1771. (e) Stevels, W. M.; Ankone, M. J. K.; Dijkstra, P. J.; Feijin, J. *Makromol. Chem. Phys.* **1995,** *196*, 1153. (f) Shen, Y.; Shen, Z.; Zhang, Y.; Yao, K. *Macromolecules* **1996,** *29*, 8289.

(4) (a) McLain, S. J.; Drysdale, N. E. *Polym. Prepr. (Am. Chem. Soc., Div. Polm. Chem.)* **1992**, *33*, 174. (b) Yamashita, M.; Takemoto, Y.; Ihara, E.; Yasuda, H. *Macromolecules* **1996,** *29*, 1798. (c) Stevels, W. M.; Ankone, M. J. K.; Dijkstra, P. J.; Feijen, J. *Macromolecules* **1996,** *29*, 8296. (d) Shen, Y.; Shen, Z.; Shen, J.; Zhang, Y.; Yao, K. *Macromolecules* **1996,** *29*, 3441.

(5) Chamberlain, B. M.; Sun, Y.; Hagadorn, J. R.; Hemmesch, E. W.; Young, V. G., Jr.; Pink, M.; Hillmyer, M. A.; Tolman, W. B. *Macromolecules* **1999,** *32*, 2400.

(6) At conversions below 90%, the PDI values for aluminum alkoxide complexes are generally below 1.2. See: Kowalski, A.; Duda, A.; Penczek, S. *Macromolecules* **1998**, *31*, 2114.

(7) Baran, J.; Duda, A.; Kowalski, A.; Szymanski, R.; Penczek, S. *Macromol. Rapid Commun.* **1997,** *18*, 325.

(8) We cannot rule out some initiation of polymerization by alkoxide arms of the macrocyclic ligand in the complexes described in this paper.

(9) The polymerization of L-lactide with tin(II) 2-ethyhexanoate in 1,4-dioxane also proceeds until a certain conversion is reached, $[M]_{eq}$. Thus, semilogarithmic plots are linear, provided that kinetic equations include $[M]_{eq}$ and that $\ln [([M]_0 - [M]_{eq})/([M]_t - [M]_{eq})]$ is plotted as a function of time. Using data in Duda, A.; Penczek, S. *Macromolecules* **1990**, *23*, 1636, the equilibrium concentration of lactide for a polymerization at 20 °C was calculated to be 0.012 M, in fair agreement with the observed equilibrium concentration of monomer in our polymerizations (0.047 M).

(10) In this polymerization, the measured equilibrium concentration of lactide was 0.15 M. This does not compare well with the value determined for the polymerization of LA with **3** ($[M]_{eq} = 0.047$ M). We expected the equilibrium concentration to be a constant at fixed temperature, and at this time we are unable to explain the source of this discrepancy.

(11) By ^{1}H NMR spectroscopy ($CDCl_3$, 25 °C), resonances for oligomeric species could not be differentiated from those of PCL.

(12) Since M_n steadily increased at short reaction times, these polymerizations were run for 16 h.

(13) Dubois, Ph.; Jacobs, C.; Jérôme, R.; Teyssié *Macromolecules* **1991**, *24*, 2266.

(14) Duda, A.; Penczek, S. *Macromol. Rapid Commun.* **1994**, *15*, 559.

(15) Reference 13 and (a) Duda, A.; Penczek, S. *Polym. Prepr. (Am. Chem. Soc. Div. Polym. Chem)* **1990,** *31*, 12. (b) Ouhadi, T.; Hamitou, A.; Jérôme, R.; Teyssié, Ph. *Macromolecules* **1976,** *9*, 927. (c) Penczek, S.; Duda, A.; Biela, T. *Polym. Prepr. (Am. Chem. Soc. Div. Polym. Chem)* **1994,** *35*, 508.

(16) Perrin, D. D.; Armarego, W. L. *Purification of Laboratory Chemicals*; Pergamon Press: New York, 1988.

(17) SHELXTL-Plus V5.0, Siemens Industrial Automation, Inc., Madison, WI.

MA0000834